2020-01-1503 Published 30 Sep 2020

Robust Development of Electric Powertrain NVH for Compact Electric SUV

Tae-Won Ha, Jin-Wook Huh, Sang-Kyu Choi, Dong-Wook Min, and Chang-Kook Chae Hyundai Motor Company

Annabel Abdy, Carsten Schmitt, Hanafy Mahmoud, Sharad Jain, and Leon Rodrigues Romax Technology

Citation: Ha, T.-W., Huh, J.-W., Choi, S.-K., Min, D.-W. et al., "Robust Development of Electric Powertrain NVH for Compact Electric SUV," SAE Technical Paper 2020-01-1503, 2020, doi:10.4271/2020-01-1503.

Abstract

Electric vehicles (EV's) present new challenges to achieving the required noise, vibration & harshness performance (NVH) compared with conventional vehicles. Specifically, high-frequency noise and unexpected noise phenomenon, previously masked by the internal combustion engine can cause annoyance in an EV. Electric motor (E-motor) whine noise caused by electromagnetic excitation during E-motor operation is caused by torque ripple and radial excitation. Under high speed and high load operating conditions, the overall sound level may be low, however high frequency whine noise can impair the vehicle level NVH performance. An example of a previously masked unexpected noise phenomenon is a droning noise that can be caused by manufacturing quality variation of the spline coupling between the rotor shaft of the E-motor and the input shaft of the reducer. It is dominated by multiple higher orders of the E-motor rotation frequency.

In this study, the high speed and high load condition whine noise problem was reproduced through electromagnetic and structural analysis. The countermeasures (E-motor geometry refinements to reduce the excitations and mechanical system transfer path modifications to reduce the vibration response) were defined and the effects investigated. Mechanical system modification to improve NVH performance without increasing the mass is challenging. However, E-motor air-gap geometry optimization, such as slot opening modulation and rotor notch modifications achieved significant noise reduction without critical trade-off of other performance.

This paper also describes the basic improvement plan proposed through the simulation of the droning noise behavior. The main two manufacturing errors (pitch error in the spline coupling and the alignment error between the rotor and the gearbox shafts) that are responsible for the unexpected droning noise were identified. Using simulation it was shown that the droning noise can be reduced through improved quality control and tolerance design optimization of factors such as axis self-alignment and spline gear tooth quality.

Introduction

In order to improve the NVH performance of a vehicle powertrain, design changes to both the source of the excitation and the structural components of the system may be necessary. If NVH issues are identified late in the production phase, making significant changes in either of these areas could lead to large system level changes or make design targets such as packaging or weight, difficult to achieve. In order to fully incorporate the interaction of the two contributing factors early in the design phase and prevent these major changes being needed at a late stage, a computer aided engineering (CAE) approach is required using a full system model, along with expertise in NVH behavior, E-motor analysis and gear-train analysis.

Understanding how excitations from the powertrain, which can be electromagnetic or mechanical in nature transmit through the system and radiate noise from the structure is required in order to be able to optimize the powertrain for noise and efficiency without compromising performance. There is currently a high focus in this area in the literature, for example reduction of cogging torque in the electrical machine in a HEV by optimizing rotor and stator notches, demonstrating in test a reduction in cabin noise in the vehicle [1]. A permanent magnet (PM) assisted synchronous reluctance machine, was designed in order to reduce particular air gap flux density harmonics, the work utilized finite element analysis (FEA) in order to capture the transfer of excitations to the powertrain, modal response of the stator and housing and the subsequent impact on the noise field around the E-motor [2]. It describes an analysis tool and process that can be used for gaining valuable insight into how the parameters in a powertrain design influence the vibration from that structure[3] and how this toolset can be used to show the user the response of the system from particular harmonics of excitation (in this case, additional harmonics caused by unbalanced magnetic pull) [4]. In [9], minimal design changes were made to the machine design, however, the effect of these on subsequent noise from the powertrain was not analyzed; tests were

required to understand whether this method was successful in reducing noise. Heavy-weight FEA models were required in order to assess the success of the design changes for reducing noise and a fairly major change was made to the rotor design concept to gain this improvement.

In the case of the system presented in the first part of this paper, where strict design constraints needed to be adhered to, the most successful way of reducing levels of vibration from the electric powertrain unit (e-PT) was found to lie with changing the source of the excitation deep within the machine design. The current paper utilizes the toolset and methodology described in [3] and presents results of the simulation validated by test. The previously published methodology has been expanded to include a prediction of radiated noise and electric machine optimization. The optimization was achieved with a combination of two methods: Slot opening modulation (SOM) and four rotor notches (FRN), these methods are similar to those presented in [6] and [9].

The following sections explain the methodology followed and demonstrate that reduction in NVH levels were successfully achieved without requiring large system level design changes. The second part of this paper describes how a multibody dynamic model was used to successfully identify that a droning noise was caused by manufacturing errors in a spline coupling.

Overview of the Electric Powertrain System NVH Issue

The Electric Powertrain has a common layout for an electrical vehicle - with a two stage parallel gearbox and an internal permanent magnet synchronous electric motor with skewed rotor. A combination of simulation and tests of the unit had identified noise issues which needed addressing, however system level design changes were not possible so a solution needed to be found that:

1. Achieved significant noise reduction
2. Didn't have any detrimental effect on weight or performance (e.g. torque, efficiency)
3. Did not require major manufacturing changes to be made to the system.

In order to achieve this, the root cause of the noise issue needed to be identified and an intelligent solution found.

E-Motor Whining Noise

Full electro-mechanical system NVH simulation using Romax Evolve employs a combination of modeling techniques selected to minimize the size and complexity of the model by only including details that are absolutely necessary for the required analysis [9]. Therefore, finite element (FE) representations of the housings and stator structure are included to accurately capture 3D deflections, whereas Timoshenko beam elements are used to represent shafts, capturing bending in a sufficient level of detail. The electrical machine rotor comprises mass and inertia, applied to the rotor shaft. Unbalance and torque ripple excitation are applied to the rotor. Non-linearity of the bearing is included in static analysis in the form of non-linear 5-DoF matrices.

The first step in the mechanical analysis process, shown in Figure 1 is to carry out a static analysis of the whole system under a particular loading condition. As the bearings are represented by non-linear stiffnesses, the static solution requires the use of iterative techniques implemented in the static solver. The outcome gives the deflections of all components and the stiffness of the system in the static deflected condition. The stiffness matrix is linearized around the static deflected condition in order to create the dynamic model. Undamped natural frequencies and mode shapes are found using the eigenvalue solver. Modal superposition is used to calculate the system response to excitations, therefore a sufficiently large number of natural frequencies are found to ensure that all modes that may affect system behavior in the frequency range of interest are identified. Constant modal damping of 2% has been used across the operating speed range. In order to run harmonic response analysis, the system needs to be excited. The NVH excitations from the E-motor were calculated using electromagnetic FE models. The two main sources of excitation in E-motors are torque ripple and radial forces acting on the stator teeth [5, 7]. Both the stator radial and tangential excitations are applied to each of the stator teeth.

The operation of a permanent magnet electrical machine is well known; in E-motor operation, alternating current is supplied to windings on the stator inducing a rotating electromagnetic field in the machine, the interaction of this field with the field created by the magnets on the rotor gives rise to shear stress in the air gap (see Figure 2). The air gap shear stress can be decomposed into radial and tangential components of which the tangential component provides a DC torque [5], and a periodic torque ripple which is dependent on many factors such as pole and magnet number and magnet and stator teeth geometry. The radial component acts to pull the rotor and stator together. The time-varying stresses on the stator teeth exhibit a complex periodic distribution in space and time.

FIGURE 1 Workflow

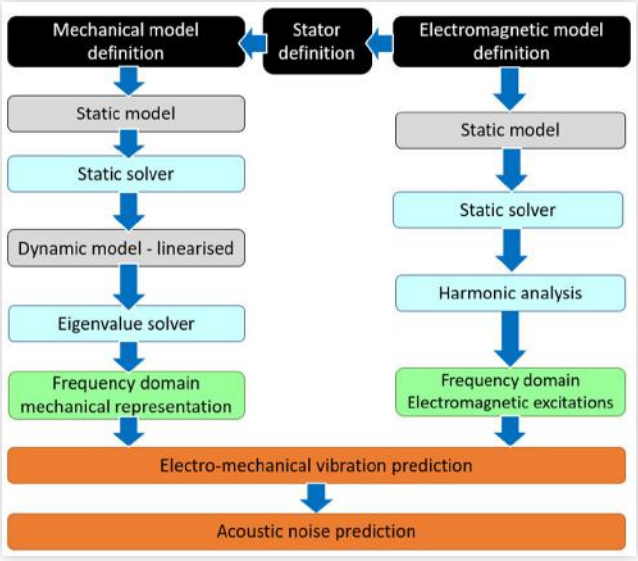

FIGURE 2 Electromagnetic Modeling

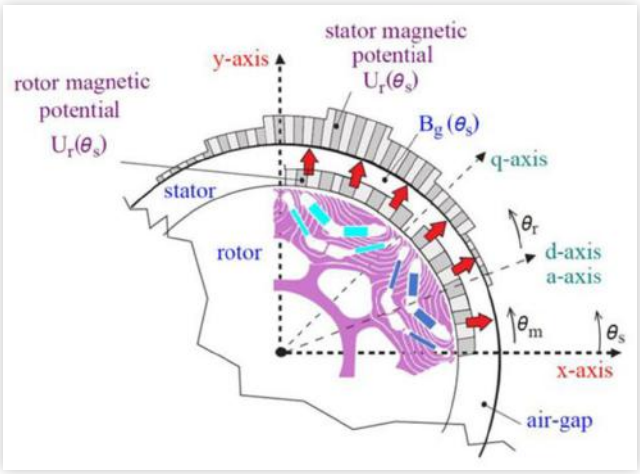

The electromagnetic forces are calculated with an electromagnetic finite element (EM FE) software package using a static time stepping approach. It is assumed the rotor and stator remain concentric, the effect of rotor skew is accounted for. Although periodicity is used in the machine model to reduce computation within the FEA ultimately, a value of rotor torque, and radial force for each tooth in the stator is calculated at every step as the rotor traverses one mechanical period.

Harmonic analysis of the time stepping torque and force data obtained from the EM FE simulation is performed. The resulting electromagnetic excitations are applied to the mechanical model as radial and tangential frequency domain forces that act on the stator teeth, and a frequency domain torsional excitation that acts on the rotor shaft. The analysis accounts for the transfer paths that exist between all excitations and vibrational response of the housing surface. To generate system response in the form of a 'speed sweep', the dynamic model is solved at discrete speeds across the drivetrain operating range. Acoustic analysis is then used to predict radiated sound power from the powertrain housing and inform the directivity of radiated noise. Acoustic analysis involves identifying the source of the excitation (electrical machine excitation in this case), a frequency range, interval step size and microphone positions. A shrink-wrap mesh is then generated, on which the noise level is predicted. The calculated data consists of pressure amplitudes and phases at each microphone position for each frequency and each excitation order. The pressures at every microphone are also used to calculate the total sound power generated at each frequency by assuming an area associated with every microphone. It is assumed that microphones are arranged on a sphere around the FE component and that every microphone represents an equal area.

For this study, operating conditions are shown in Table 1 were simulated in order to compare to test correlation.

Test Methodology Two sets of tests were carried out, frequency response function (FRF) tests and dyno based NVH tests. The dyno tests were carried out on the fully assembled powertrain unit without reducer. This was operated across

TABLE 1 Operating Conditions used for E-motor Excitation Calculation

Torque [Nm]	Speed [rpm]
395	2000, 4000
190	2000, 4000, 6000, 8000
130	2000, 4000, 6000, 8000, 9000
-100	2000, 4000, 6000, 8000, 10000

the full range of torque and speed and accelerometer responses were obtained. The FRF tests were conducted on an E-motor housing sub-assembly (sub-assembly simulation models for modal analysis are shown in Figure 3), test hardware included accelerometers which were specified to achieve reasonable accuracy up to 5kHz. The sensor and excitation positions were selected based on modal analysis results from FEA. The final stage of correlation was carried out for the housing with stator and covers see Figure 4.

Correlation Results The first level of correlation was achieved from matching natural frequencies from the FRF tests with those obtained from FE modal analysis. This was carried out for all mentioned components. The natural frequency correlation exercise gives good confidence in the model and in using this for investigation of the noise problem.

Table 2 presents the natural frequencies for stator and sub-assembly structure. A very good level of correlation was achieved up to 5kHz. The largest deviation between frequencies is less than 5%. In some cases, a number of modes shapes have very similar natural frequencies, a well-known phenomenon due to the symmetry in the structure [11]. The different modes can be differentiated in the simulation, however, the mode shapes and frequencies of these groups of modes are too similar to be individually identified from the measurement data and are therefore denoted 'Not identified' in the table. It

FIGURE 3 Components Selected for Experimental Modal Analysis

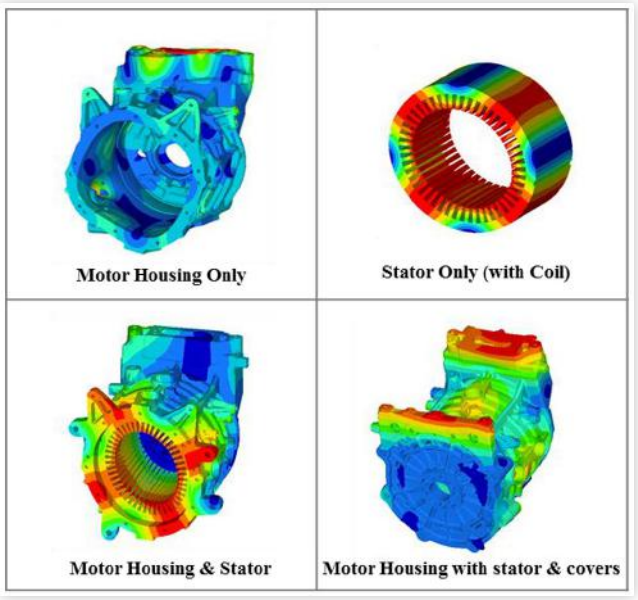

FIGURE 4 FE Housing with Stator and Covers Used for Final Stage of Correlation.

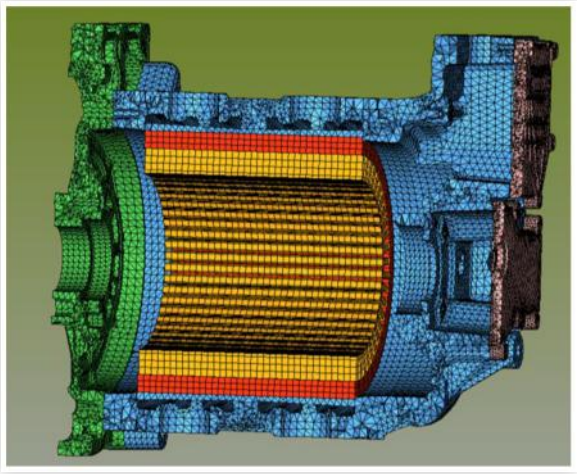

was not expected that good correlation would be achieved above 5kHz due to the specification of the accelerometers and model reduction techniques used in order to run the analysis. Issues with these methods cause well known uncertainties in both experimental and analysis results. The natural frequency correlation exercise gives good confidence in the model and in using this for investigation of the noise problem. From the tests, the 48th order excitation (which would have come from the e-machine) was identified as problematic (See Figure 5).

TABLE 2 Natural Frequencies Obtained by FRF

Stator only(with coil)			
Mode index	Test [Hz]	Simulation [Hz]	Deviation [%]
1	660	655	0.76
2	Not identified	666	n/a
3	Not identified	729	n/a
4	755	734	2.65
9	1705	1729	1.17
6	Not identified	1753	n/a
7	1795	1825	1.39
8	Not identified	1843	n/a
9	2525	2592	2.57
10	2630	2600	1.14
11	Not identified	3008	n/a
12	Not identified	3044	n/a
13	Not identified	3079	n/a
14	3250	3100	4.62
15	3450	3424	0.87
16	3555	3582	0.70
17	Not identified	3595	n/a
18	Not identified	3955	n/a
19	Not identified	3955	n/a
20	Not identified	3960	n/a
21	4020	3965	1.37

TABLE 2 (Continued) Natural Frequencies Obtained by FRF

Motor Housing with stator & covers			
Mode index	Test [Hz]	Simulation [Hz]	Deviation [%]
1	1410	1420	0.71
2	1460	1450	0.68
3	1760	Does not exist	n/a
4	1790	Docs not exist	n/a
5	2100	2005	4.52
6	2260	2280	0.88
7	Not identified	2291	n/a
8	2430	2500	2.88
9	2500	2545	1.80
10	2580	2570	0.39
11	2680	2665	0.56
12	2805	2805	0.00
13	2930	2855	2.56
14	Not identified	2940	n/a
15	2950	2955	0.17
16	2975	2975	0.00
17	3170	Does not exist	n/a
18	3380	Does not exist	n/a
19	3470	3475	0.14
20	3530	3525	0.14
21	3610	3575	0.97
22	3665	3630	0.95
23	Not identified	3695	n/a
24	3730	3745	0.40
25	3820	3795	0.65
26	3905	3945	1.02
27	4005	3975	0.75
28	4130	4155	0.61
29	4230	4210	0.47
30	4320	4310	0.23
31	Not identified	4345	n/a
32	4360	4375	0.34
33	4420	4490	1.58
34	4550	4605	1.21
35	4610	4640	0.65
36	4745	4765	0.42
37	4800	4805	0.10
38	4910	4875	0.71
39	4980	4975	0.10
40	5030	5025	0.10
41	5130	5125	0.10
42	Not identified	5170	n/a
43	5215	5212	0.06

Figure 6 & Figure 7 show a comparison of the acceleration test results (blue line) with the simulation (red line) for the 24th and 48th order. A good level of correlation was achieved up to 7000rpm which is the region where tests were carried out at a constant torque of 190Nm. The close correlation

FIGURE 5 Vehicle Test Results

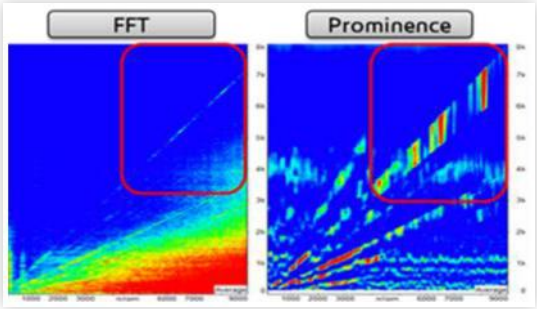

FIGURE 6 Test Response vs Simulation Response *(24th order)*

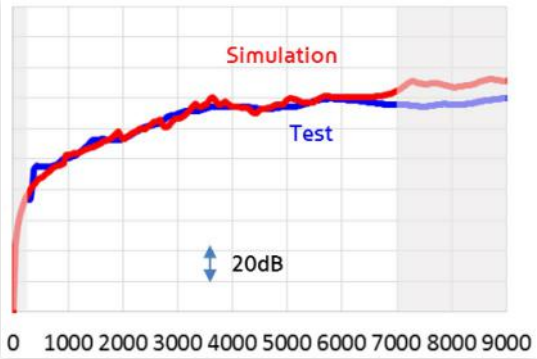

FIGURE 7 Test Response vs Simulation Response *(48th order)*

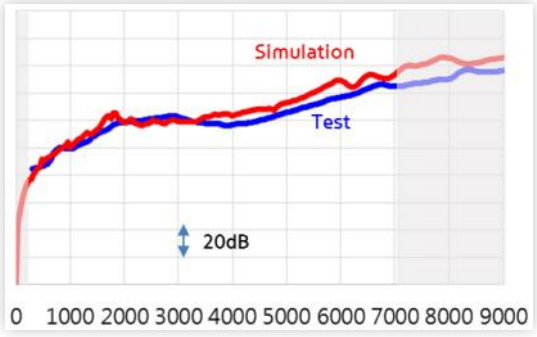

between test and simulation indicates the assumptions made in the simulation model, such as 2% constant damping are appropriate for representing this system. As speed increased from 7000rpm, the torque level of the test machine dropped but simulated torque remained at 190Nm, therefore, correlation cannot be made for the higher speed results.

The actual operating deflected shape of the system can be visualized and the mechanism of noise transfer understood with the Evolve model. Examples are shown in Figure 8. In order to further understand the contribution of the different components of E-motor excitation, analysis was run with each excitation in isolation. It was seen that there was a significant difference in the magnitudes of the harmonics in the lead and lag sections of the skewed machine. Due to this effect, the lead end of the machine may see a significantly larger excitation than the lag section. In some cases, it is also possible to see a different response in the forward and reverse direction because the lead and lag sections would reverse in orientation to the direction of rotation. Figure 9 shows that below 5500rpm the response due to 'lead only' torque ripple and 'lag only' torque ripple is actually higher than the response due to the combined lead and lag torque ripple showing a cancelling effect. Figure 10 shows that the peak in response at 8000rpm is dominated by the radial force excitation.

Optimization of E-Motor NVH Once the system model was built and validated and the noise source fully understood, optimization of the design could be carried out in order to mitigate the issues found.

Structural Modification Some small design changes were made to the housing including the rear covers as well as the housing sides. These modifications were constrained by weight restrictions which stipulated that there must be no increase in weight of the housing component. Ribs were added

FIGURE 8 Operating Deflection Shape Results

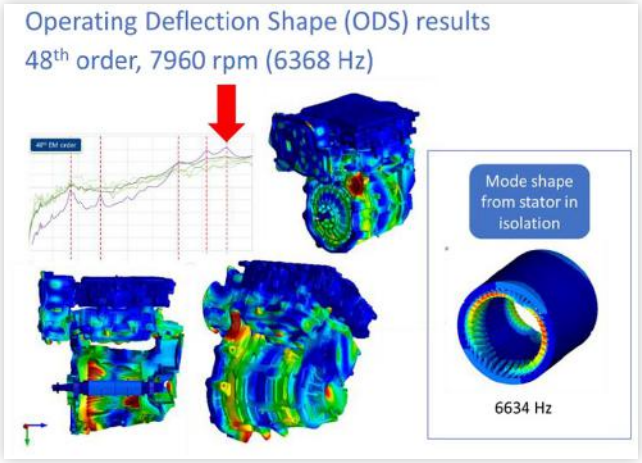

FIGURE 9 Torque Ripple Contribution to Response

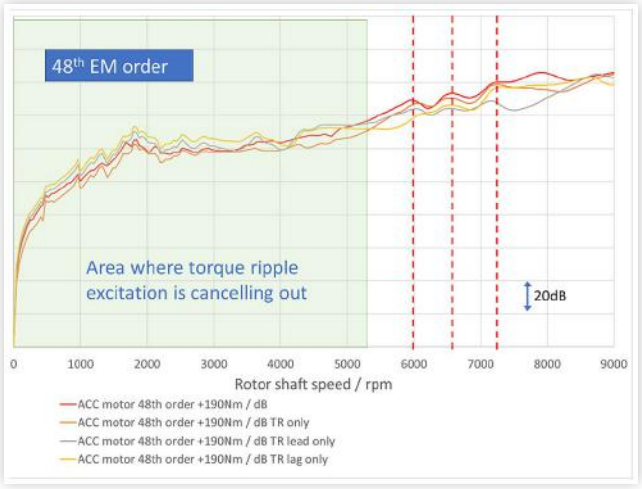

FIGURE 10 Radial Force Contribution to Response

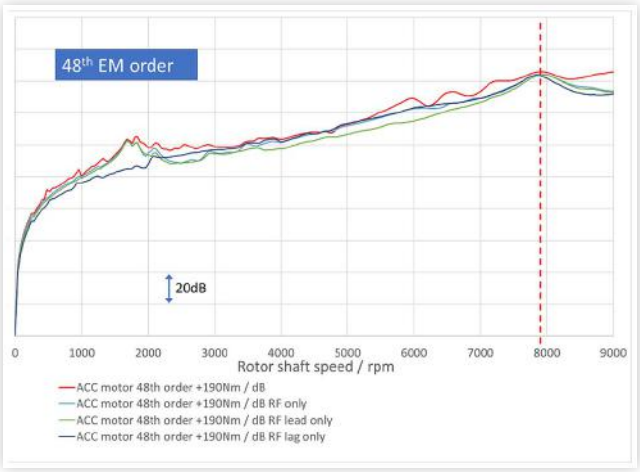

to stiffen some areas and material was removed in other areas to compensate for the mass increase caused by the additional ribs.

In order to verify that the changes made to the housing did not have a detrimental effect on the static deflections and misalignments in the gearbox, the simulation model was expanded to include the gearbox and final drive. The full system model was not only used to check the static behavior of the gearbox but was also used for the spline droning noise simulations described later in this paper. In addition to predicting the system vibration response at the accelerometer locations, the simulation model was also used to predict the acoustic sound field. Figure 11 shows the sound pressure and power level Campbell diagrams generated and the graphical representation of directivity enabling an improved understanding of the most prominent directions for acoustic emission. Figure 12 shows the detailed predicted sound pressure level at specific microphone locations. Although the types of changes made at this stage might be typical solutions that may be applied in any industry when NVH issues are found in the testing stage of development, the analysis found only minor improvement from these changes. This confirmed the need for a system level e-NVH solution including optimization of the E-motor excitations as focusing only on the mechanical aspects of the design may not always provide a satisfactory solution.

E-Machine Design Optimization

E-Machine Design Optimization Methodology. The excitations in an electrical machine are a function of the airgap flux density. This can be broken down into individual stator and rotor scalar magnetic potential or magneto motive force (MMF). In a linear model the stator and rotor components of the airgap flux density can be calculated using superposition as illustrated in Figure 13. The combination of stator and rotor MMF harmonics can be altered in such a way as to reduce the magnitude of the problematic harmonic. This can be achieved by modifying the MMF waveform of the stator or the rotor or both. In this study, the electric machine excitation reduction focused on two methods: Slot opening

FIGURE 11 Sound Power and Pressure Campbell Diagrams and Directivity

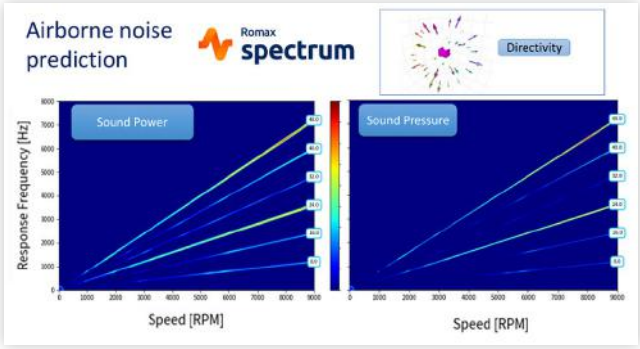

FIGURE 12 Detailed Comparison of the Predicted Sound Pressure at Specific Microphone Positions

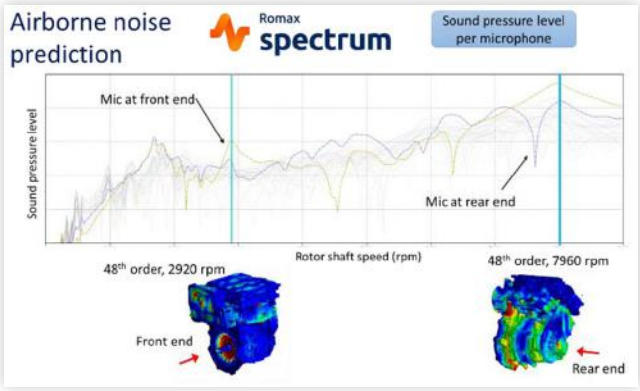

FIGURE 13 EM Optimization Workflow

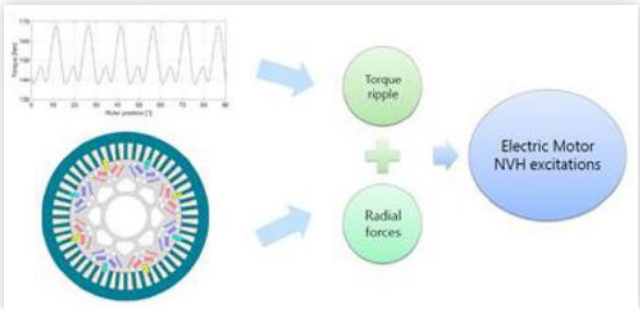

modulation (SOM); Four rotor notches (FRN), and a combination of these methods. Figure 14 shows the changes that can be made with the SOM method. Electromagnetic finite element analysis was used for the optimization. An optimization algorithm was used in this approach, with the objective to avoid fundamental changes in machine performance (e.g. torque, efficiency) or type of machine.

E-Machine Design Optimization Results. A combination of the SOM method and FRN method enabled significant machine excitation reduction in critical areas. Figure 15 shows that a 7 dB airborne noise reduction was achieved for the 48th order radial and torque ripple excitation at 190

FIGURE 14 EM Optimization Parameters

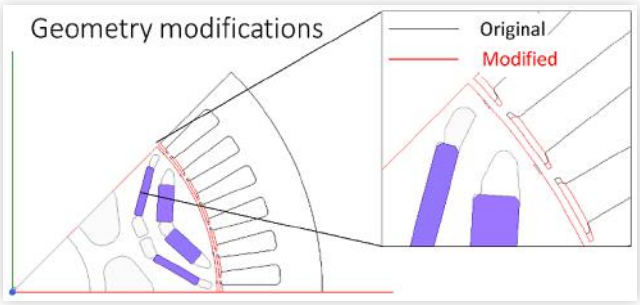

FIGURE 15 Optimization Results

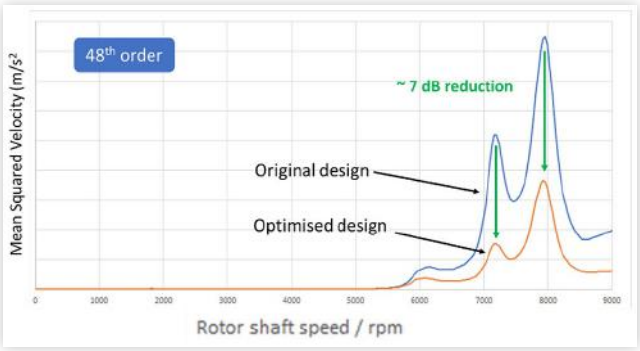

Nm, when comparing system response from initial machine excitation with system response from optimized machine excitation at higher speeds. Static torque, efficiency and temperatures were also maintained within the stringent targets. The design changes did lead to an increase in EM excitation for some other load cases, however, when system level analysis was carried out, it was found that this increase was not problematic as the response amplitudes to those excitations were low.

Conclusion to E-Motor Whining Noise Investigation

This study has shown that good correlation has been achieved between the simulation model and test results for the natural frequencies of the components and subcomponents in the drivetrain. It has also identified that 48th order electromagnetic excitation dominates the vibration response of the system, which matches the test result. From the drivetrain system model, unique insight has been gained regarding the transfer of the source of the vibration through to the response of the system across the frequency range of interest, demonstrating the value of a full system electromagnetic-mechanical model of the drivetrain for understanding the NVH behavior. Such a system can be created before a structure is built and tested and used for design modifications and optimization early in the development phase, reducing development time and risk that costly redesigns are required if problems are only identified once a product is tested. The current study has also illustrated the importance of simulating the relevant parameters in detail in order to identify potential for system level improvement through component level optimization. In this case, a vibration issue was identified as caused by the 48th order electromagnetic excitation; typical mechanical only solutions were found to have minimal effect on noise reduction due to the constraints imposed by the design targets. However, optimizing the internal design of the electrical machine has reduced the source of the noise with minimal impact on overall performance and no changes are required of the rest of the system.

Droning Noise of e-PT System

There was a droning noise from the e-PT system (see Figure 16) at low torque and low speed because of manufacturing quality variation at early development. Test results showed that the noise was dominated by multiple E-motor-shaft harmonics. It could also be seen that there was significant energy content in harmonics as high as 20. It was suspected that the source of the droning noise was the spline coupling connecting the E-motor shaft and gearbox input shaft. For this part of the study, a transient time-domain analysis was performed to reproduce the noise and understand the underlying behavior.

Simulation Model Development and Validation To investigate the droning noise issue, a multi-body dynamic model of the system was developed (see Figure 17). The model included the following components: Motor shaft; Gearbox input shaft; Spline coupling connecting the two shafts; Support bearings. The shafts were flexible and the bearings had non-linear clearance. The forces acting on the model were: Motor drive torque; Gear load torque - radial and axial forces; Radial excitation caused by the rotor imbalance. The load acting on the bearings caused by the thermal expansion of the shafts (20 °C ~ 90 °C) was also considered. The spline-coupling

FIGURE 16 Droning Noise of e-PT System

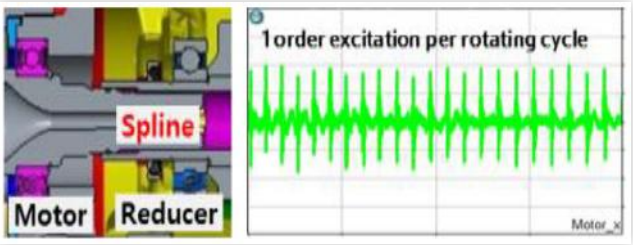

FIGURE 17 Multi-Body Dynamic Model

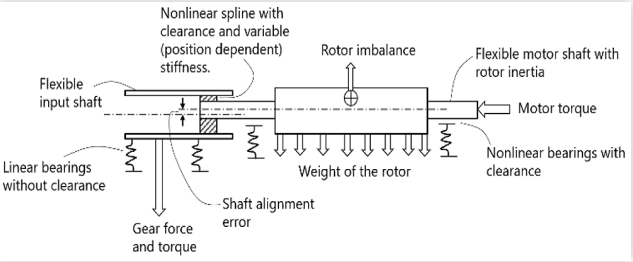

model used was non-linear and considered the following physics : Clearance between the external and internal spline teeth; Variation in tooth bending stiffness caused by the relative radial or tilt movement between external and internal spline teeth; Static alignment errors between the centers of external and internal splines; Pitch error or tooth indexing errors within the spline teeth.

Figure 18 shows how the spline force changes with the radial movement of the external spline relative to the internal. As expected, there is no force in the clearance zone. When the radial movement exceeds the clearance, there is a non-zero force. The slope of the force-displacement curve changes with displacement, which shows that the spline stiffness is a function of radial movement. The alignment error between the E-motor and gearbox shafts and the pitch error in the spline coupling were calculated for use in the analysis. The model was solved in time-domain using an Ordinary Different Equation solver to capture any transient phenomena that could potentially lead to the droning noise behavior. A speed-sweep analysis was run on the multi-body model described previously. The transient response was calculated at various locations. The following parameters were used for the analysis:

Identification Noise Mechanism Acceleration response simulation results at a bearing on the E-motor shaft are shown in Figure 19. The results show several harmonics of the shaft rotation frequency which are similar to observations in the test data. A resonance mode is seen near 400 Hz,

FIGURE 18 Spline Forces

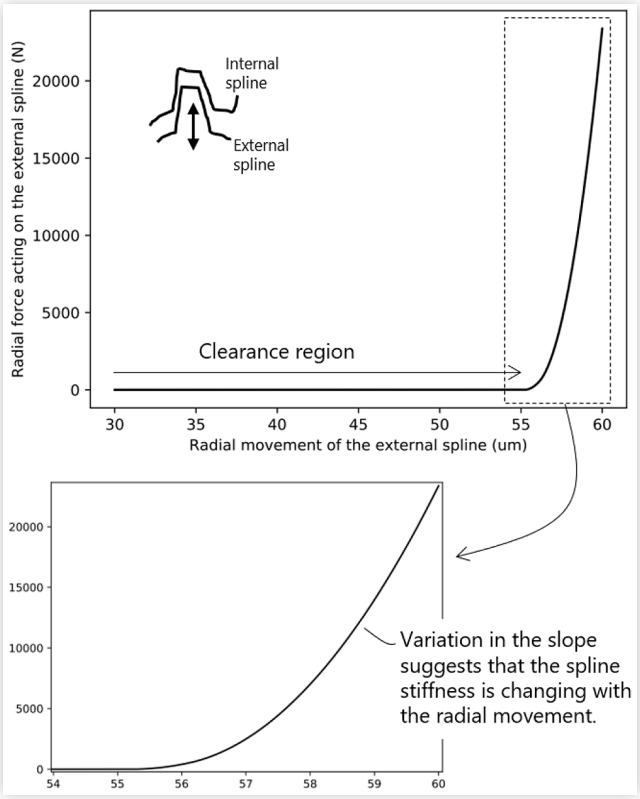

TABLE 3 Analysis Parameters

Alignment Error between motor and gearbox shafts	100 µm
Cumulative pitch error in spline coupling	20 µm
Torque Applied	30 Nm
Speed	0 ~ 2400 rpm
Duration of Simulation	30 s

with higher response when the shaft-frequency harmonics cross this resonance. The eigenvalue analysis of the system reveals that there is an E-motor shaft bending mode near 400Hz that is getting excited and hence resulting in high acceleration. This matches closely with the measured frequency spectrum test data shown in Figure 20. The acceleration time-history was converted into an audio signal and from this signal the droning noise similar to the one experienced during in-vehicle test can be heard. Having reproduced the noise successfully, the next step was to look at the influence of the shaft-alignment and spline pitch error and establish the underlying source of this noise.

Figure 21 shows the variation in the magnitudes of the motor-shaft harmonics with spline pitch and alignment errors. For 0 um pitch error, there are no peaks at the shaft rotation frequency and its harmonics. When the pitch error becomes non-zero, peaks start to appear at shaft rotation frequency and its higher harmonics. The height of these peaks increases as the magnitude of pitch error increases. So, for a higher value of pitch error, there will be a louder droning noise. And for 0 um alignment error, there are not many higher harmonics of shaft rotation frequency. There is still a peak at the shaft rotation frequency and first two

FIGURE 19 Calculated Frequency Spectrum

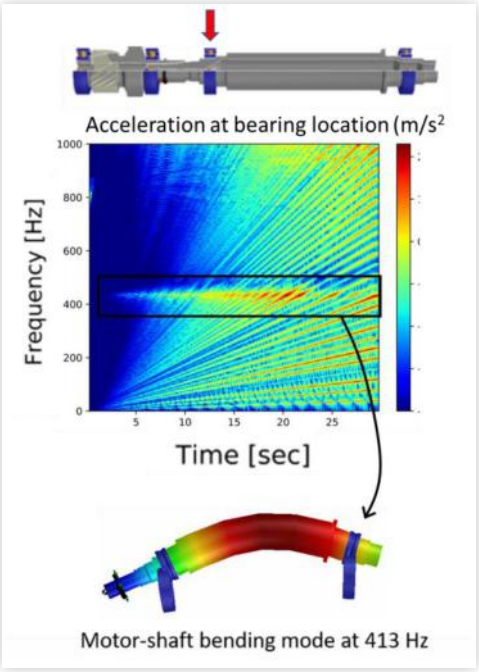

FIGURE 20 Measured Frequency Spectrum of the System

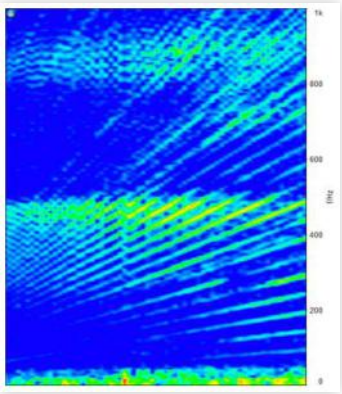

FIGURE 21 Parametric Study

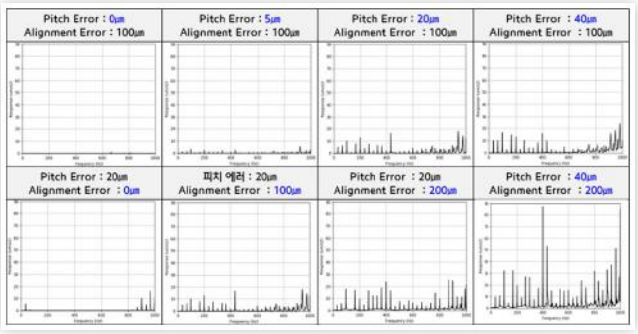

harmonics, but their energy content is quite small. The reason why there are fewer small peaks is because even though there is no alignment error between the shafts, there will still be deflections due to applied loads and there will be a small amount of angular misalignment in the spline coupling. When the alignment error becomes non-zero, higher order peaks start to appear, with significantly higher energy compared to zero-alignment case. Comparing the frequency spectrum of 100 um alignment error with 200 um, the 200 um spectrum contains higher orders with much higher energy. Therefore, similar to the influence of pitch error, droning noise becomes louder when the alignment error increases. When the pitch error is zero, the external spline's center does not move much and settles down to an equilibrium position. For non-zero pitch errors, the external spline's center shows a lot of movement and never actually settles down to an equilibrium position. The higher the pitch error, the larger the movement of spline's center. The shape of the spline's trajectory is not a smooth circle or ellipse, it is more complicated and is of much higher order (see Figure 22). This is the reason why we get so many higher harmonics with significant energy content.

As the alignment error increases, the amount with which the spline moves does not change much. However, the way the spline moves changes significantly. For the zero-alignment case, the spline's center moves in a perfect ellipse. As the alignment error increases, the trajectory starts to deviate from a perfectly smooth ellipse to a more complicated shape with higher order curves. This explains why the

FIGURE 22 Trajectories of the Center of the External Spline Relative to the Internal Spline - Simulation vs Test

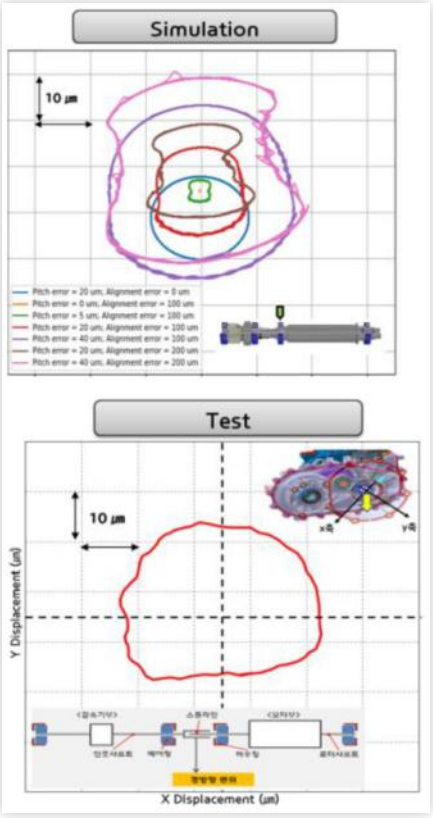

energy content of higher order harmonics increases with alignment error. Analysis results showed that the droning noise only appears when a pitch error is introduced in the spline coupling. Also, that the shaft alignment error magnifies the droning noise significantly. In order to understand why this is occurring (see Figure 23). The top image shows the hypothetical situation where no pitch error is present. In this case, all the spline teeth will be uniformly loaded and will contribute equally to the spline's stiffness. So, as teeth rotate with the spline, no change in the spline's stiffness behavior is seen. When pitch error is introduced in the spline, some teeth will carry more load than others and the teeth that carry more load will contribute more to the spline's stiffness. When these teeth are rotated, the spline stiffness behavior in the radial direction will change in a stationary reference frame. Therefore, a periodic stiffness variation is seen with periodicity equal to one spline rotation.

Conclusion to the Droning Noise Investigation

Using a multi-body dynamic model combined with manufacturing errors it was possible to replicate the droning noise experienced by tests. The noise was caused by the spline coupling and was dominated by multiple higher orders to E-motor rotation frequency content. The two manufacturing tolerances that have the most significant contribution to the droning noise are pitch error in the spline coupling and the

FIGURE 23 Understanding the Source of the Droning Noise

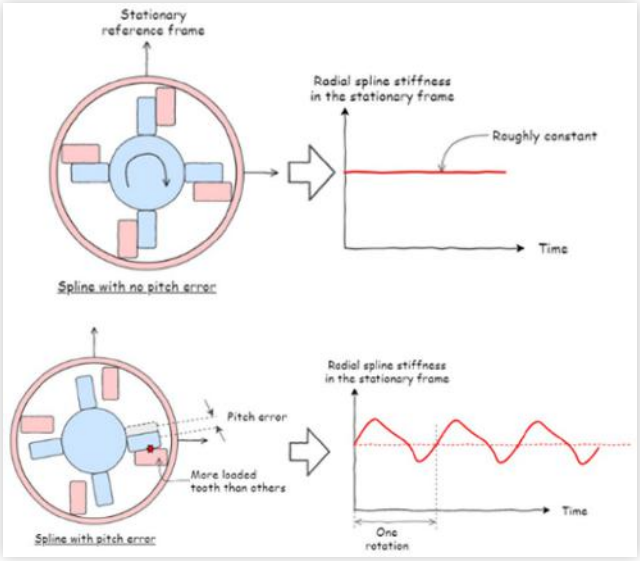

alignment error between the E-motor and the gearbox shafts. This part of the study looked at the influence of these errors on the droning noise and explained the underlying cause behind the droning noise. The cumulative pitch error in the spline coupling was reduced in order to reduce the droning noise and to tighten the tolerances so that the alignment error between the motor and gearbox shaft was reduced.

Summary

Both parts of this paper have demonstrated how component level excitation can cause noise emission from an e-PT. Detailed understanding of the workings of the individual components, whether they are mechanical or electromagnetic in nature is required as is a system level model that can predict the transfer of these excitations and resulting noise emission.

The combination of a system level modeling approach, interfacing software and engineering expertise have enabled the optimization for noise without compromising previous performance levels or requiring major re-designs.

The root cause of the unexpected droning noise due to the manufacturing errors was identified and the countermeasures for noise improvement were established.

References

1. Do, S.H., Kim, K.B., Park, J.B., Hong, N.H. et al., "Optimal Design of the 2nd Generation TMED Traction Motor," in *IEEE International Electric Machines & Drives Conference (IEMDC)*, San Diego, 2019, doi:10.1109/IEMDC.2019.8785321.
2. Zheng, H., Wei, C., Sun, D., Pei, R. et al., "Rotor Design of Permanent Magnet Synchronous Reluctance Motors in Rail Traffic Vehicle," in *21st International Conference on Electrical Machines and Systems (ICEMS)*, Jeju, South Korea, 2018, doi:10.23919/ICEMS.2018.8549125.
3. Holehouse, R., Shahaj, A., Michon, M., and James, B., "Integrated Approach to Electro-Mechanical System NVH Analysis," in *10th International Styrian Noise, Vibration & Harshness Congress: The European Automotive Noise Conference*, Graz, Austria, 2018, doi:10.4271/2018-01-14993.
4. Bombardi, F.V., Atallah, K., Shahaj, A., Michon, M. et al., "Effects of Unbalanced Magnetic Pull on NVH Performance of an Electric Drivetrain," SAE Technical Paper 2018-01-1504, 2018, https://doi.org/10.4271/2018-01-1504.
5. Yang, S.J., *Low-Noise Electrical Motors Monographs in Electrical and Electronic Engineering* (Oxford Science Publications, 1981).
6. Wu, Y.C., and Chen, Y.T., "Mitigation of Cogging Torque for Brushless Interior Permanent-Magnet Motors," *Transaction on Mechanical Engineering, International Journal of Science & Technology* 22(6):2163-2169, Dec. 2015.
7. Gieras, J.F., Wang, C., and Lai, J.C., *Noise of Polyphase Electric Motors* (Taylor & Francis Group, 2006).
8. Pina Ortega, A.J., "Fast Design of Asymmetrical Permanent Magnet Synchronous Machines that Minimize Pulsating Torque," *Electromagnetic Research B* 76:111-123, 2017.
9. Hwang, M.H., Lee, H.S., and Cha, H.R., "Analysis of Torque Ripple and Cogging Torque reduction in Electric Vehicle Traction Platform Applying Rotor Notched Design," *Energies*, 2018, doi:10.3390/en11113053.
10. Platten, M. "Dynamic Simulation of Transmissions and Drivelines Using Romax Designer," in *SIA Acoustic Simulation Workshop*, Paris, Oct. 2011.
11. Verma, S.P. "Noise and Vibrations of Electrical Machines and Drives: Their Production and Means of Reduction" in *Proceedings of the 1996 IEEE International Conference on Power Electronics, Drives and Energy Systems for Industrial Growth*, vol. 2, 1031-1037, New Delhi, India, 1996.

Contact Information

Tae-Won Ha
Hyundai Motor Company, R&D Division,
Powertrain NVH Test Team 2,
twha@hyundai.com

Acknowledgments

The authors of this paper would like to thank the other members of the project team who supported the work described in this paper and other contributors to the preparation of this paper including Rob Holehouse, Annabel Shahaj, Donmin Lee, Marek Jakubaszek, Matthew Bees & Gary Johnstone.

Definitions/Abbreviations

EV - Electric vehicle
HEV - Hybrid electric vehicle
MMF - Magneto motive force
EM - Electromagnetic
FE - Finite element
NVH - Noise, Vibration & Harshness

ISSN 0148-7191